THE JOURNAL OF BIOLOGICAL CHEMISTRY VOL. 281, NO. 25, pp. 17246–17252, June 23, 2006

A Serpin from the Gut Bacterium *Bifidobacterium longum* Inhibits Eukaryotic Elastase-like Serine Proteases*

Received for publication, February 22, 2006, and in revised form, April 19, 2006 Published, JBC Papers in Press, April 20, 2006, DOI 10.1074/jbc.M601678200

Dmitri Ivanov[1], **Celine Emonet, Francis Foata, Michael Affolter, Michelle Delley, Makda Fisseha, Stephanie Blum-Sperisen, Sunil Kochhar, and Fabrizio Arigoni**[2]

From the Nestlé Research Center, Vers-chez-les-Blanc, P. O. Box 44, CH-1000 Lausanne 26, Switzerland

Serpins form a large class of protease inhibitors involved in regulation of a wide spectrum of physiological processes. Recently identified prokaryotic members of this protein family may provide a key to the evolutionary origins of the unique serpin fold and the associated inhibitory mechanism. We performed a biochemical characterization of a serpin from *Bifidobacterium longum*, an anaerobic Gram-positive bacterium that naturally colonizes human gastrointestinal tract. The *B. longum* serpin was shown to efficiently inhibit eukaryotic elastase-like proteases with a stoichiometry of inhibition close to 1. Porcine pancreatic elastase and human neutrophil elastase were inhibited with the second order association constants of 4.7×10^4 M^{-1} s^{-1} and 2.1×10^4 M^{-1} s^{-1}, respectively. The *B. longum* serpin is expected to be active in the gastrointestinal tract, because incubation of the purified recombinant serpin with mouse feces produces a stable covalent serpin-protease adduct readily detectable by SDS-PAGE. Bifidobacteria may encounter both pancreatic elastase and neutrophil elastase in their natural habitat and protection against exogenous proteolysis may play an important role in the interaction between these commensal bacteria and their host.

Numerous signaling pathways in higher organisms, such as apoptosis, inflammation, blood clotting, and others, involve proteolytic events as mediators of signal initiation, transmission, and termination. Substrate specificity of the involved proteases and a tight regulation of their activation and inhibition are essential regulatory mechanisms of temporal and spatial control in proteolytic signaling. Serpins (serine protease inhibitors) represent a large class of polypeptide serine protease inhibitors that are involved in regulation of a wide spectrum of protease-mediated processes (1, 2). They fold into a metastable native structure with an exposed substrate-like reactive center loop (RCL)[3] (3) and, unlike the small polypeptide inhibitors from the Kunitz or Kazal family, they do not act as reversible competitive inhibitors of the target proteases but rather as stoichiometric suicide inactivators with a unique inhibition mechanism driven by conformational change. Upon cleavage of RCL by the target protease and formation of the covalent acyl-enzyme reaction intermediate, the serpin fold undergoes a major conformational rearrangement, and the RCL is inserted as the middle strand of the beta sheet A to form a six-stranded anti-parallel β sheet at the core of the cleaved serpin structure (4). This conformational change creates a steric clash with the protease and the resulting distortion inactivates the enzyme and traps it as a covalent serpin-protease adduct (5).

Serpins are widely distributed in higher eukaryotic organisms and are also found in some viruses where they appear to modulate virus-host interactions and viral infectivity (1). Thirty-four serpins identified in the human genome belong to nine different phylogenetic clades in the currently adopted serpin classification (2). Notably, some members of the serpin superfamily, such as ovalbumin, angiotensin, and others (6, 7), do not act as protease inhibitors but rather perform non-inhibitory biological functions despite a clear evolutionary relationship and an almost identical native fold. These non-inhibitory members of the serpin superfamily appear to be incapable of the structural rearrangement required for protease inhibition (8).

Recently serpins were identified in bacteria and archea expanding their presence to all major domains of life (9, 10). This observation suggests that the unique serpin fold and the associated inhibitory mechanism may have originated at the early stages of evolution. Very little is currently known about the function of serpins in prokaryotes (11). The sequence-based analysis suggests that prokaryotic members of the serpin superfamily are functional protease inhibitors, and a serpin from *Thermobifida fusca*, thermopin, was shown to inhibit chymotrypsin albeit by means of an unconventional cleavage site (12). Thermopin is, however, unusual because of its ability to function at elevated temperature, whereas conventional serpins are prone to polymerization at higher temperature due to the metastable nature of their native fold (13).

Here we present a biochemical characterization of the prokaryotic serpin identified in the genome of *Bifidobacterium longum* NCC2705, an infant-derived strain of bifidobacteria (10). Bifidobacteria are Gram-positive anaerobes that naturally colonize the gastrointestinal tract (GIT) of mammals and are considered to play an important role in promoting a healthy GIT. Little is known about the interaction mechanisms between the bifidobacteria and their host, but recent data indicate that the beneficial properties of bifidobacteria for treatment of irritable bowel disease and ulcerative colitis appear to be related to the immune-modulating properties of these organisms (14, 15). The sequencing of the *B. longum* genome revealed a genetic makeup that reflected a remarkable adaptation of this organism to the GIT environment. Intriguingly, the genome-wide search for predicted secreted proteins identified a serpin-like molecule encoded by this microorganism (10). To explore the physiological role of this *B. longum* protein in the GIT environment and its possible function in host-bacterium cross-talk, we performed a biochemical characterization of this hypothetical serpin.

EXPERIMENTAL PROCEDURES

Enzymes, Inhibitors, and Substrates—The following enzymes and reagents were used: bovine pancreatic α-chymotrypsin, porcine pancreatic trypsin, and porcine pancreatic elastase (Fluka, now Sigma); subtili-

* The costs of publication of this article were defrayed in part by the payment of page charges. This article must therefore be hereby marked "*advertisement*" in accordance with 18 U.S.C. Section 1734 solely to indicate this fact.

[1] To whom correspondence may be addressed: Dept. of Biological Chemistry and Molecular Pharmacology, Harvard Medical School, 240 Longwood Ave., Boston MA 02140. Tel.: 617-432-3211; Fax: 617-432-4383; E-mail: dmitri_ivanov@hms.harvard.edu.

[2] To whom correspondence may be addressed. Tel.: 41-21-785-83-64; Fax: 41-21-785-85-44; E-mail: fabrizio.arigoni@rdls.nestle.com.

[3] The abbreviations used are: RCL, reactive center loop; GIT, gastrointestinal tract; HNE, human neutrophil elastase; PPE, porcine pancreatic elastase; SI, stoichiometry of inhibition; MCA, 7-amido-4-methyl coumarin; AMC, amino-4-methyl coumarin; Dnp, 2,4-dinitrophenyl; MeOSuc, methyl-*O*-succinyl; MS, mass spectrometry; MALDI-TOF, matrix-assisted laser desorption ionization time-of-flight; Nval, norvaline.

sin Carlsberg, papain (from papaya latex), and human neutrophil elastase (human leukocyte elastase) (Sigma); cathepsin G (human neutrophil) (Athens Research and Technology, Athens, GA); MeOSuc-AAPV-AMC and MeOSuc-AAPA-chloromethylketone (Bachem AG, Bubendorf, Switzerland); and MCA-RPKPVE-Nval-WRK(Dnp)-NH_2 and human α_1-antitrypsin (*SERPIN A1*) (R&D Systems, Minneapolis, MN).

Production of B. longum serpin in Escherichia coli—The serpin gene (*BL0108*) from *B. longum* without the sequence encoding the N-terminal hydrophobic domain (amino acids 1–40) was cloned into the Gateway expression vector pDEST17 (Invitrogen). The final construct contained a 22 amino acid N-terminal extension (MSYY-HHHHHHLESTSLYKKAGF) with a His_6 tag for affinity purification. The *E. coli* BL21S1 cells were transformed using the standard protocol (Invitrogen). Cells were grown in M9 minimal medium containing 100 mg/liter of ampicillin, and protein expression was induced by addition of 0.1 mM isopropyl β-D-thiogalactopyranoside. For production of ^{15}N-labeled protein, 1 g of $^{15}NH_4Cl$ was used as the sole nitrogen source in M9 medium.

Protein Purification—Frozen cells from 1 liter of bacterial culture were resuspended in 50 ml of lysis buffer (50 mM sodium phosphate, pH 7.2, 200 mM NaCl, 0.2 mM Pefabloc, 1 mg/ml lysozyme, 10 μg/ml DNase I), and lysed by sonication. The cell debris were cleared by centrifugation at 10,000 × *g* for 30 min. The protein was purified on a 5-ml HiTrap chelating HP column (Amerhsam Biosciences) charged with Ni^{2+} ions using the standard protocol. After the imidazole gradient elution the protein was further purified by size-exclusion chromatography using a HiLoad 26/60 Superdex 75 gel filtration column (Amersham Biosciences) and a 50 mM sodium phosphate, pH 7.2, 100 mM NaCl buffer.

Survey of B. longum Serpin Inhibitory Activity—All reactions were performed in 50 mM sodium phosphate, pH 7.2, 100 mM NaCl buffer with the exception of human neutrophil elastase, which was assayed in 50 mM Tris-HCl, pH 8.0, 500 mM NaCl buffer. The stock solutions of fluorogenic peptide substrates were prepared in Me_2SO and stored at −40 °C. The Me_2SO substrate stocks were diluted ~100-fold into reaction buffers to prepare 2× substrate buffers (20 μM for MCA-RPKPVE-Nval-WRK(Dnp)-NH_2; 400 μM for MeOSuc-AAPV-AMC and MeOSuc-AAPF-AMC). The enzymes were then incubated for 40 min with various amounts of serpin (20 nM to 10 μM). The enzymatic activity was subsequently assayed by rapidly mixing 50 μl of the substrate buffer with 50 μl of the enzyme/serpin solution in a 96-well clear bottom plates and recording the fluorescence change on a FLEXStation fluorescence plate reader (Molecular Devices Corp., Sunnyvale, CA).

Kinetics of Inhibition—The kinetic parameters of serpin inhibition were determined by the progress curve method (16, 17). The enzymes and the substrates were dissolved in reaction buffers. Various amounts of serpin were added to the substrate solution to yield final concentrations of ~2–10-fold excess over the enzyme concentration. The substrate/serpin and the enzyme solutions were incubated at 37 °C for 10 min, and then 50 μl of each were rapidly mixed, and the progress curve fluorescence readings were recorded at 37 °C. The first-order association rates k_{obs} were determined by non-linear regression fitting of the progress curve data using Equation 1.

$$P = (v_0/k_{obs})(1 - e^{(-k_{obs} \cdot t)}) \quad \text{(Eq. 1)}$$

The initial rate (v_0) was determined from the progress curve at zero serpin concentration. For experiments where excess of serpin over the protease was too low to ensure validity of the pseudo first-order approximation, only the initial parts of the progress curves were used for non-linear regression fitting of k_{obs}. The apparent second-order association constant was determined as the slope of the k_{obs} *versus* [I] plot ($k'_{app} = \Delta k_{obs}/\Delta[I]$), where [I] is the corresponding serpin concentration. The second-order association rate was then corrected taking into account that the serpin and the fluorescent substrate compete for the active site of the protease: $k_a = (1 + [S]/K_M)\, k'_{app}$, where [S] is substrate concentration, and the K_m of the enzyme for the substrate was determined from the Lineweaver-Burk plot. MeOSuc-AAPV-AMC K_m was 362 μM for human neutrophil elastase (HNE) and 275 μM for porcine pancreatic elastase (PPE).

Stoichiometry of Inhibition (SI), Covalent Serpin-Protease Adduct, and the Cleavage Site—Protein concentrations were determined using theoretically calculated extinction coefficients at 280 nm: 54,390 M^{-1} cm^{-1} (PPE), 20,100 M^{-1} cm^{-1} (HNE), and 59,150 M^{-1} cm^{-1} (*B. longum* serpin). Proteases were also titrated with stoichiometric activators: PPE with MeOSuc-AAPA-chloromethylketone and HNE with α_1-antitrypsin. Enzyme concentrations determined by such titration were within 15% from the values determined by the A_{280} measurements.

Covalent protease-serpin adducts were prepared by incubation of 10 μM solutions of serpin with varying amounts of protease (2.5, 5, 10, and 20 μM) in the standard reaction buffers. After 5-min incubation at room temperature 50 μM AEBSF (Sigma) was added to the mixtures, and the samples were analyzed by SDS-PAGE. The content of the bands of the Coomassie-stained gel was identified using tandem MS analysis by NanoLC-ESI-MS/MS on a Finnigan LCQ classic ion trap (Thermo, San Jose, CA) (18).

Cleavage Site—The RCL cleavage site was determined by MALDI-MS analysis of the peptide fragments after incubation of serpin with proteases. The 20 μM serpin and 10 μM protease mixture was incubated for 5 min in the reaction buffer at room temperature. The masses of the peptide fragments were determined by MALDI-MS (Bruker Autoflex ToF) in linear mode (19).

Incubation of Serpin with Fecal Proteins—Feces from axenic mice were resuspended in 1× phosphate-buffered saline with glass beads (Sigma G4649) and lysed in a Beadbeater (Mini-Beadbeater, BioSpec Products). The debris and the glass beads were removed by centrifugation at 12,000 rpm for 10 min. Purified serpin (10 ng) was incubated 10 min at room temperature with different amounts of fecal proteins and then mixed with 4× sample buffer and boiled for 5 min. Protein samples were separated by SDS-PAGE and transferred to pure nitrocellulose membrane (0.2 μm; Bio-Rad) using standard methods. The membrane was blocked for 60 min with 5% skimmed milk in 1× Tris-buffered saline and probed with rabbit anti *B. longum* serpin antibodies diluted 1:3000. The antigen-antibody complex was detected with a goat anti-rabbit IgG conjugated to horseradish peroxidase (Bio-Rad; diluted 1:3000) using the BM chemiluminescence substrate from Roche Applied Science.

RESULTS

Primary Sequence Analysis of B. longum Serpin—The BLASTP program (20) was used to search for the closest homologues of the predicted *B. longum* serpin (BL0108) in the non-redundant protein data base of National Center for Biotechnology Information. The sequence alignment with several representative serpin sequences returned by the BLASTP query is shown in Fig. 1. Current serpin classification divides serpin sequences into clades based on their phylogenetic relationships (21), with members of the same clade defined by the normalized BLAST score of larger than 279 bits (2). The highest similarity score observed for *B. longum* serpin homologues returned by BLAST is 139 bits ($E = 2e^{-31}$, ~28% sequence identity), which qualifies *B. longum* serpin as an orphan in the current classification. Most of the top 10 matches in the BLASTP query are serpins from other prokaryotic species, two of which are shown in

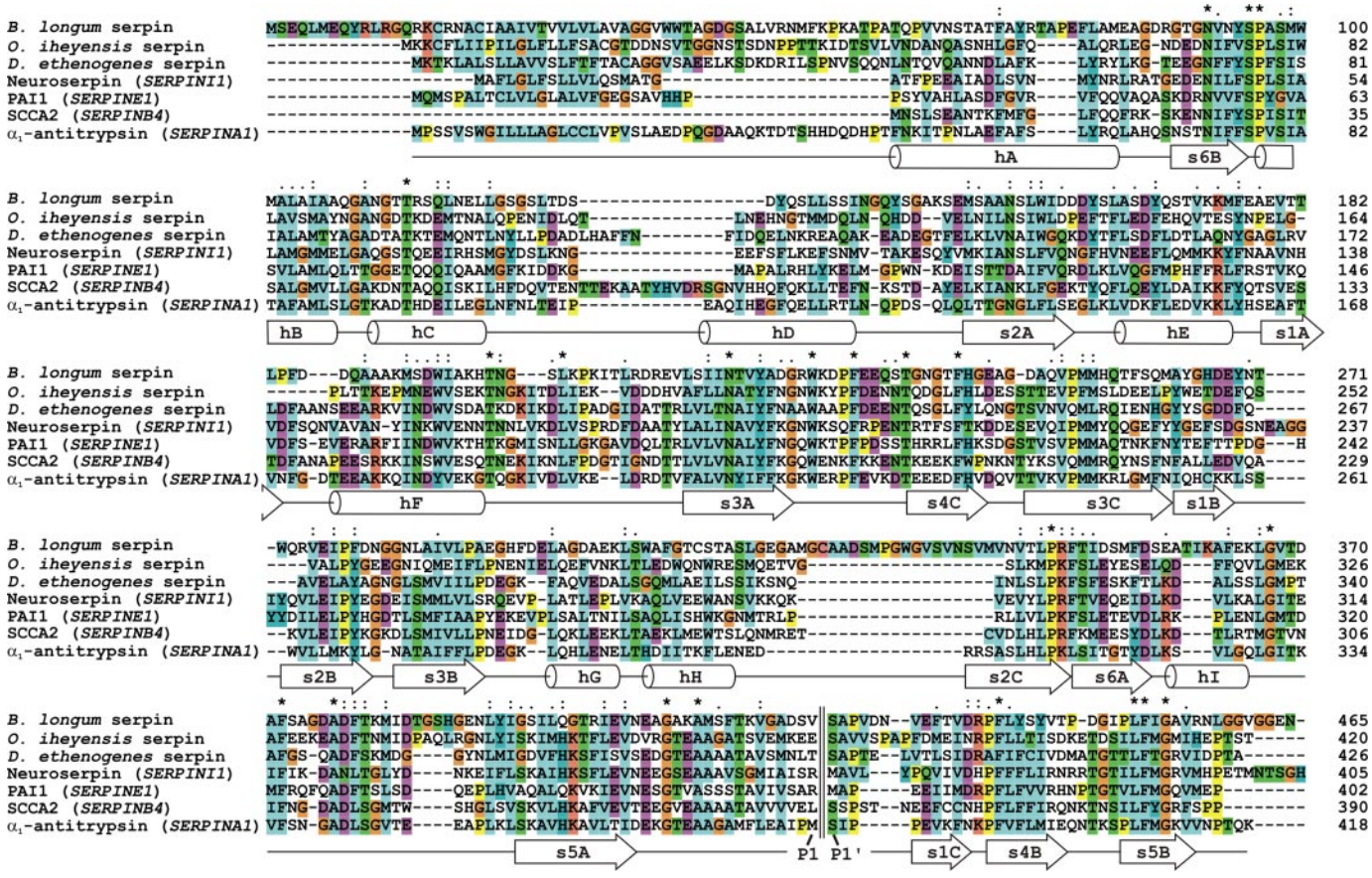

FIGURE 1. **Multiple sequence alignment of *B. longum* serpin with other known serpin sequences.** Shown are *Oceanobacillus iheyensis HTE831* serpin (GenBank™ accession number: NP_694094, normalized BLAST score: 139 bits), *Dehalococcoides ethenogenes 195* serpin (GenBank™ accession number: YP_180970, 134 bits), neuroserpin (*SERPINI1*, GenBank™ accession number: NP_005016, 120 bits), plasminogen activator inhibitor 1 (*SERPINE1*,GenBank™ accession number: P05121, 116 bits), squamous cell carcinoma antigen 2 (*SERPINB4*, GenBank™ accession number: P48594, 112 bits), and α_1-antitrypsin (*SERPINA1*,GenBank™ accession number: P01009, 82.8 bits). Alignment was produced using ClustalW (1.82) webserver. The residues are colored based on the residue type to visualize the conserved patterns. The secondary structure elements of the conserved serpin fold are shown below the alignment and are based on the native *SERPINA1* structure (Protein Data Bank ID: 1QLP). The predicted cleavage site is marked with a *double vertical line*. P1 and P1′ positions of the reactive center loop are labeled.

TABLE 1
Survey of protease inhibition by *B. longum* serpin

Protease (final concentration)	*B. longum* serpin (maximum concentration)	Inhibition	Substrate (final concentration)
α-Chymotrypsin (50 nM)	5 μM	No	MCA-RPKPVE-Nval-WRK(Dnp)-NH_2 (10 μM)
Trypsin (50 nM)	5 μM	No	MCA-RPKPVE-Nval-WRK(Dnp)-NH_2 (10 μM)
Subtilisin Carlsberg (50 nM)	5 μM	No	MCA-RPKPVE-Nval-WRK(Dnp)-NH_2 (10 μM)
Pancreatic elastase PPE (50 nM)	0.13 μM	100%	MeOSuc-AAPV-AMC (200 μM)
Neutrophil elastase HNE (100 nM)	1 μM	100%	MeOSuc-AAPV-AMC (200 μM)
Cathepsin G (170 nM)	10 μM	No	MeOSuc-AAPF-AMC (200 μM)
Papain (8 μM)	16 μM	No	MeOSuc-AAPF-AMC (200 μM)

Fig. 1, while the closest homologues from eukaryotic serpin clades return BLAST scores below 120 bits (Fig. 1).

The *B. longum* serpin is predicted to contain all secondary structure elements of the conserved serpin fold and is therefore expected to form a stably folded, functional protein. Analysis of the RCL alignment predicts that the cleaved bond of the *B. longum* serpin is located between valine and serine (Fig. 1).

Purification of B. longum Serpin and Survey of Inhibitory Activity—The serpin encoded by *B. longum* was predicted by TMHMM (22) to be directed to the membrane via its N-terminal hydrohphobic region and to be exposed on the surface of *B. longum* cells. The DNA sequence encoding the core serpin domain without the predicted hydrophobic domain (amino acids 1–40) was cloned into an *E. coli* expression vector and the protein was purified as described under "Experimental Procedures." The expressed protein was predominantly soluble, and protein purification yielded more than 10 mg of protein per liter of culture. The purified protein was more than 95% pure by SDS-PAGE analysis.

To experimentally verify that the *B. longum* serpin is indeed an inhibitory serpin as suggested by its primary sequence analysis, we screened for its inhibitory activity against a selection of proteases (Table 1). The proteases were incubated with varied amounts of serpin for 40 min, after which the residual protease activity was assayed by detecting hydrolysis of fluorogenic substrates. *B. longum* serpin was found to inhibit proteases from the elastase family, which is consistent with the presence of a valine residue in the P1 position of the reactive center loop. Complete inhibition was observed for porcine pancreatic elastase and human neutrophil elastase after incubation with excess amounts of *B. longum* serpin. No other proteases included in the screen showed any statistically

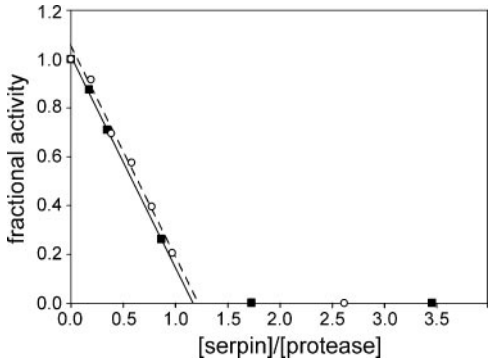

FIGURE 2. **Stoichiometric protease inhibition by *B. longum* serpin.** Fractional activity of PPE (—■—) and of HNE (—○—) measured after incubation with various concentrations of *B. longum* serpin.

significant degree of inhibition. Notably, the observed inhibition profile of the *B. longum* serpin is distinct from the inhibition profile of the physiological serpin inhibitors of human neutrophil elastase. α_1-Antitrypsin (*SERPINA1*), for example, is also known to inhibit trypsin, while monocyte/neutrophil elastase inhibitor (*SERPINB1*) acts as an efficient cathepsin G inhibitor. Differences in the RCL composition, which affect targeting of proteases to the correct cleavage site, are likely to be responsible for the distinct inhibition profiles of these serpins. Indeed, trypsin appears to cleave *B. longum* serpin at an RCL site not compatible with inhibition (see below).

B. longum Serpin Acts as a Stoichiometric Covalent Inactivator—To demonstrate that *B. longum* serpin inhibits target proteases via a classic stoichiometric inactivation mechanism, activities of PPE, and HNE were measured after incubation with various amounts of serpin. The linear decrease of activity observed for both proteases was consistent with the stoichiometric inactivation mechanism of serpin inhibition (Fig. 2). The SI was determined to be close to 1.

To demonstrate the covalent nature of inhibition, we investigated whether a stable covalent adduct of the serpin with the protease could be identified by SDS-PAGE. A fixed amount of serpin (10 μM) was incubated with various amounts of PPE and HNE, and the products of the reaction were analyzed by SDS-PAGE and coomassie staining (Fig. 3, *A* and *B*). Protein bands of higher molecular weight indicative of the covalent serpin-protease adduct are readily visible on the gel after the incubation of the serpin with each of the two proteases. More than one band appeared at higher molecular weight values when compared with the band of the pure serpin alone. To further characterize the bands we performed tandem mass spectrometry (MS-MS) identification of their protein content (Fig. 3*C*). The serpin amino acid sequence and the SWISSPROT data base were used for analysis of the MS-MS data by SEQUEST program (Thermo Finnigan). Bands 3 and 5 (Fig. 3*A*) were clearly identified as pure serpin and pure PPE respectively, with 10 peptides matched in each case. When the serpin was incubated with increasing amounts of the protease, the pure serpin band (*band 3*, Fig. 3*A*) disappeared as new bands (*bands 1*, *2*, and *4*) emerged. *Band 4* most likely corresponds to cleaved serpin, since only one PPE peptide matched to this band indicating that low amounts of the protease were present (if any). In contrast, *bands 1* and *2* (Fig. 3, *A* and *C*) were both clearly identified as covalent adducts of the serpin with the protease. Very similar results were obtained with human neutrophil elastase (Fig. 3, *B* and *C*). Semiquantitative estimate of the band intensities is consistent with the SI value of 2 or less, which agrees well with our titration experiments. Multiple adduct bands may be due to the fact that the protease is destabilized in the covalent complex and is therefore susceptible to proteolysis. Alternatively the band mobility on the gel may be

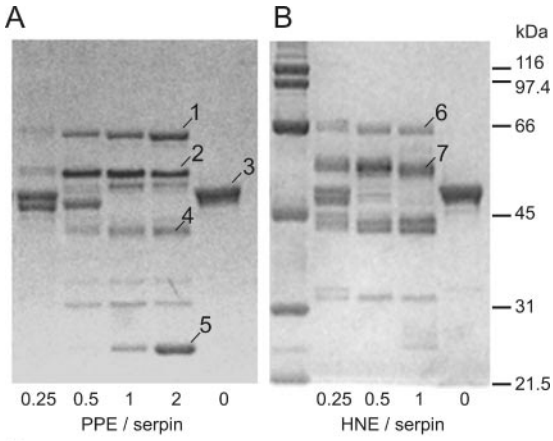

C

Band	Protein ID by MS-MS	Number of Peptides matched
1	*B.longum* serpin ELA1_PIG	5 6
2	*B.longum* serpin ELA1_PIG	8 6
3	*B.longum* serpin	10
4	*B.longum* serpin ELA1_PIG	6 1
5	ELA1_PIG ELA2_PIG	10 3
6	*B.longum* serpin ELNE_HUMAN	6 2
7	*B.longum* serpin ELNE_HUMAN	6 5

FIGURE 3. ***B. longum* serpin forms a stable covalent adduct with the target proteases.** *A* and *B*, SDS-PAGE analysis of 10-μl samples after incubation of serpin with PPE and HNE. *A*, serpin concentration: 10 μM; PPE concentrations, 2.5, 5, 10, and 20 μM. *B*, serpin concentration: 10 μM; HNE concentrations: 2.5, 5, and 10 μM. The protease/serpin ratios are shown below the corresponding lanes. The *right lane* in both gels contained 10 μl of the 10 μM solution of the purified *B. longum* serpin and no protease. *C*, MS-MS identification of the protein bands labeled in *A* and *B*. The table shows the names of the matched proteins and the number of distinct peptide fragments identified after the tryptic digestion. SWISSPROT names are listed for the matched proteases.

affected by the incomplete unfolding of the serpin, which adopts an extremely stable conformation upon cleavage. The latter explanation is supported by the observation that mobility of band 2 depended on the duration and the temperature of the sample treatment in the loading buffer before SDS-PAGE (data not shown).

Second-order Association Constants—The second-order association constants for PPE and HNE inhibition by *B. longum* serpin were determined by the progress curve method (Fig. 4). The measured rate of the serpin-HNE association ($k_a = 4.7 \times 10^4\ \mathrm{M}^{-1}\ \mathrm{s}^{-1}$) was similar to the rate of serpin-PPE association ($k_a = 2.1 \times 10^4\ \mathrm{M}^{-1}\ \mathrm{s}^{-1}$). For comparison α_1-antitrypsin inhibits HNE and PPE with the association rates of $k_a = 6.5 \times 10^7\ \mathrm{M}^{-1}\ \mathrm{s}^{-1}$ and $k_a = 1.0 \times 10^5\ \mathrm{M}^{-1}\ \mathrm{s}^{-1}$, respectively (23).

Cleavage Site—Finally, we checked whether pancreatic elastase and neutrophil elastase cleave the predicted P1-P1′ bond of the reactive center loop. When the protease is trapped by the serpin in the acyl-enzyme intermediate, the cleaved-off N-terminal segment of the serpin is no longer covalently attached to the protein and can be analyzed by mass spectrometry. The molecular mass of this cleaved N-terminal peptide can be used to determine location of the cleavage site. The *B. longum* serpin was incubated with the enzymes for 10 min at room temperature and the molecular weight of the formed peptide fragments were determined by MALDI-MS (Fig. 5). In addition to PPE and HNE, we also analyzed cleavage products after incubation with trypsin, for which no inhibition was observed in our titration assays. Once again

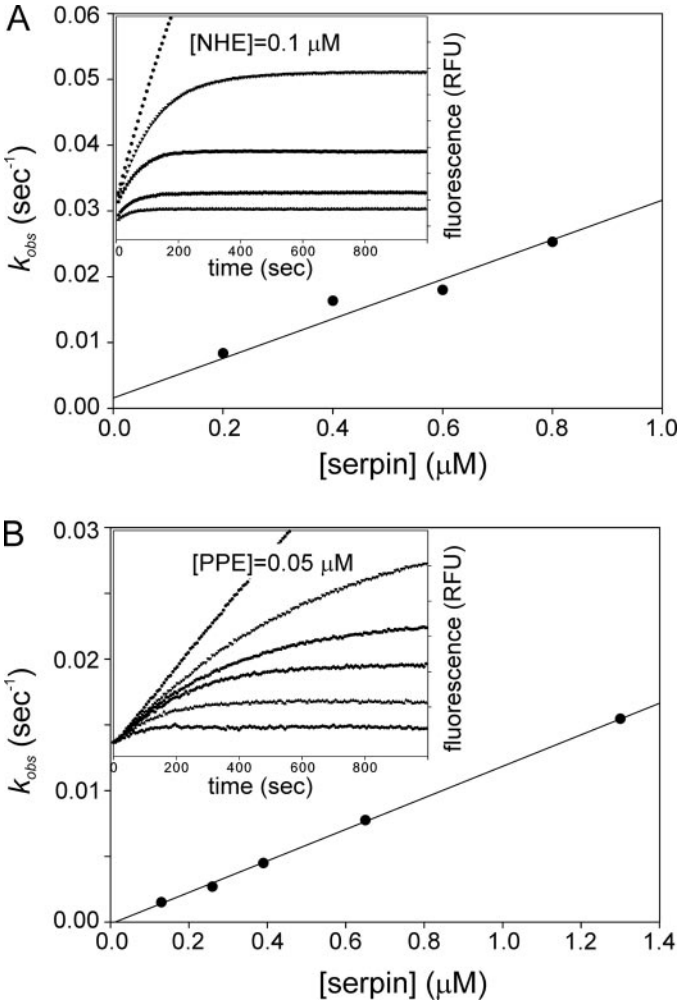

FIGURE 4. **Kinetics of protease inhibition by *B. longum* serpin.** *A*, human neutrophil elastase inhibition. Final HNE concentration in all reaction mixtures was 0.1 μM and final serpin concentrations were 0.2, 0.4, 0.6, and 0.8 μM. *B*, porcine pancreatic elastase inhibition. PPE concentration: 0.05 μM; serpin concentrations: 0.13, 0.26, 0.39, 0.65, and 1.3 μM. The observed pseudo first-order inhibition constants are plotted as a function of the serpin concentration. The second-order association constants were determined from the slope of the plots by linear regression (*solid lines*). The raw progress curve data are shown in the *insets*.

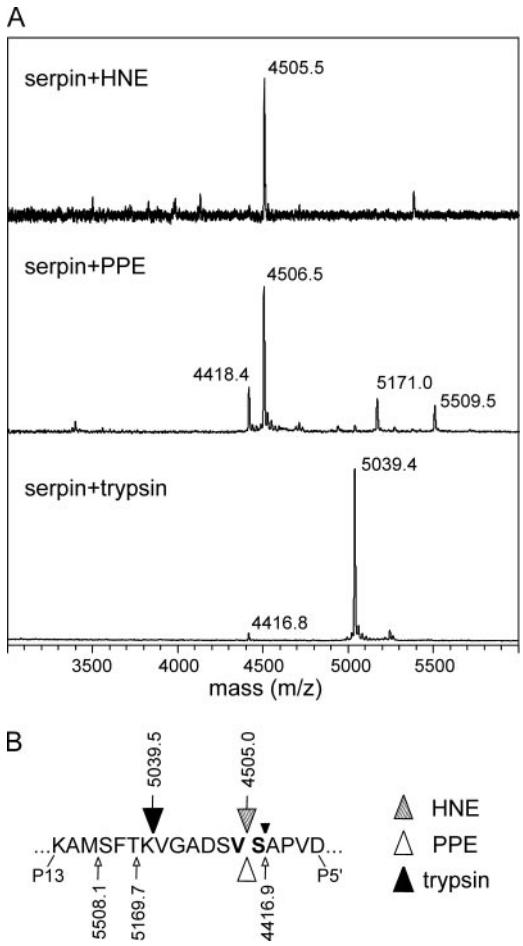

FIGURE 5. **Identification of the serpin cleavage site.** *A*, MALDI-MS analysis of the peptide fragments after incubation of serpin with human neutrophil elastase (*top*), porcine pancreatic elastase (*middle*), and trypsin (*bottom*). The experimentally determined masses (MH^+) are shown above the corresponding peaks. *B*, diagram of the reactive center loop showing the major (*large triangles*) and minor (*small triangles*) cleavage sites identified by the MALDI-MS analysis. The cleavage sites are labeled with the predicted fragment masses (MH^+) calculated for uniformly ^{15}N-labeled *B. longum* serpin. Valine 423 and serine 424 in the P1 and the P1′ position, respectively, are shown in *bold*.

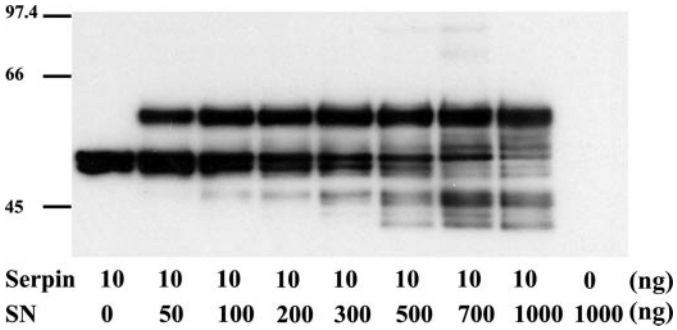

FIGURE 6. **A serpin-protease covalent adduct is formed in mouse feces.** *B. longum serpin* was incubated with increasing amounts of fecal proteins, separated by SDS-PAGE, and analyzed by Western blot with rabbit anti-serpin antibodies. A serpin immunoreactive band of higher molecular mass than the free serpin is revealed when serpin and the fecal extract were mixed. The amount of proteins in the sample mix is given below the figure. Serpin refers to the purified *B. longum* serpin, *SN* refers to protein extract obtained from mouse feces.

100% uniformly ^{15}N-labeled serpin was used in these experiments. For HNE the molecular mass (MH^+) of the major fragment was 4505.6, which is a very good match for the theoretical (MH^+) value of 4506.0 predicted for the P1-P1′ cleavage site in the ^{15}N-labeled protein. This peptide was also the major fragment observed for porcine pancreatic elastase, although several minor fragments corresponding to different cleavage sites were also observed. For trypsin the primary cleavage site was determined to be between Lys^{381} and Val^{382}. This observation explains the lack of *B. longum* inhibitory activity against trypsin, as the correct length of the cleaved reactive center loop is critical for formation of the stable covalent adduct. This is supported by the SDS-PAGE analysis, which shows accumulation of the cleaved serpin band after incubation of serpin with trypsin (data not shown).

Serpin Activity in Mammalian Feces—To test whether the inhibitory activity of the *B. longum* serpin observed *in vitro* is relevant within the mammalian gastrointestinal tract we incubated the purified recombinant *B. longum* serpin with a crude protein extract obtained from mouse feces. After incubation, the samples were analyzed by SDS-PAGE and Western blotting (Fig. 6). The gel shows that upon addition of increasing amounts of the mouse fecal extract the free serpin band gradually disappears while a heavier immunoreactive band emerges indicative of a covalent adduct formed by the serpin with one or more proteases present in the feces. Most of the serpin in this experiment appears to be trapped in the covalent adduct with a target protease while very little

unproductive serpin cleavage (immunoreactive bands of lower molecular weight) is observed. This result suggests that the secreted *B. longum* serpin would be an efficient inhibitor within mammalian GIT and demonstrates that serpin-reactive proteases are present in the mouse feces.

DISCUSSION

Despite the extensive knowledge about the role of serpins in regulation of the protease-mediated processes in higher multicellular eukaryotes, very little is currently known about their function in prokaryotes. The presence of serpins in bacteria and archea implies that this protein superfamily is likely to have originated before the separation of the major branches of life. However, serpins are rather sparsely present among the prokaryotes indicating that they are either easily lost when not essential for survival or alternatively that they may have been acquired by prokaryotes as the result of horizontal gene transfer. Most of the serpins from unicellular organisms are distantly related to the serpins from higher organisms and do not belong to any of the existing serpin clades. This also applies to the *B. longum* serpin, which is an orphan in the current serpin classification. These observations suggest that if unicellular serpins were acquired by horizontal gene transfer, such events would have occurred independently for different serpins, and the original multicellular donors of these genes are not present in the existing genomic databases (11). The ability of prokaryotic serpins to undergo reactive center loop insertion was predicted from the sequence analysis of their RCL hinge regions (9, 11), but until now biochemical data were available for only one prokaryotic serpin, thermopin (12). Thermopin was found to inhibit chymotrypsin with a SI of 8.0 ± 0.1 and an apparent (non-SI-corrected) second-order rate constant (k_{app}) of $8.4 \pm 0.4 \times 10^4\ M^{-1}\ s^{-1}$. However, the inhibition was not achieved by the cleavage of the predicted P1-P1′ bond (12). In contrast to the unusual cleavage pattern observed for thermopin we find that *B. longum* serpin inhibits elastase-like serine proteases following conventional cleavage of the P1-P1′ bond with a stoichiometry of inhibition close to 1. When combined with the primary sequence analysis of the unicellular serpins (11) the conventional inhibitory activity of the *B. longum* serpin suggests that the majority of serpins identified in unicellular genomes are inhibitory proteins with the inhibition mechanism identical to that of the inhibitory serpins in higher multicellular eukaryotes. Our findings indicate that the inhibitory function of serpins either evolved very early in the course of evolution or (in the case of the horizontal gene transfer scenario) that the inhibitory function of the serpins was predominant in the multicellular organims by the time horizontal gene transfers occurred.

Bifidobacteria are commensal bacteria that naturally colonize the colon of humans and other mammals. We have demonstrated that the *B. longum* NCC2705 serpin is an efficient inhibitor of pancreatic elastase and neutrophil elastase, which appears relevant given that bifidobacteria are likely to be in contact with both of these enzymes in the gastrointestinal tract. Pancreatic elastase is a digestive enzyme secreted by the acinar cells in the pancreas, and unlike other pancreatic enzymes it is very stable during the passage through the intestine as its activity can readily be detected in the feces (24). Protease inhibitors produced by bacteria may act to protect them against exogenous proteases and to provide an important competitive advantage. For example, secreted protease inhibitors identified in *Bacillus brevis* and *Privotella intermedia* are thought to protect these organisms against external proteolytic attack (25, 26), while the periplasmic protease inhibitor of *E. coli* ecotin was shown to protect these bacteria against neutrophil elastase (27). The observed association constants of *B. longum* serpin with human neutrophil elastase and porcine pancreatic elastase were $4.7 \times 10^4\ M^{-1}\ s^{-1}$ and $2.1 \times 10^4\ M^{-1}\ s^{-1}$, respectively. These values are 3 orders of magnitude lower than the association rate of $6.5 \times 10^7\ M^{-1}\ s^{-1}$ reported for HNE inhibition by α_1-antitrypsin (23). The remarkably high efficiency of the serpins in the blood plasma is required to ensure less than 100 ms inhibition lifetime to provide effective control of the target protease (28), while outside of the actively circulated blood stream the physiologically relevant values for the association rates would naturally be much lower. We hypothesize that the kinetic constants determined for *B. longum* serpin should be sufficient to provide adequate protease inhibition for bacterial species that inhabit the gastrointestinal tract. Incubation of the recombinant serpin with mouse feces rapidly leads to formation of a covalent adduct of the serpin with an unidentified protease present in the feces. This demonstrates that the secreted serpin would act as an efficient inhibitor in the GIT because very little non-productive serpin degradation by non-target proteases (such as trypsin) is observed in this experiment. We note that the target protease or proteases are quite abundant in the mouse feces, an observation that suggests that the observed covalent adduct is most likely formed with the pancreatic elastase.

The potential health-promoting effects of bifidobacteria are widely discussed in the literature, and bifidobacteria are frequently included as part of commercial preparations aimed to restore a healthy balance in intestinal microflora (14, 15, 29, 30). The healthy commensal flora required for normal intestinal function involves a delicate homeostatic balance on the mucosal surfaces of the gastrointestinal tract manifested in the apparent tolerance of the immune system toward commensal microorganisms, whereas pathological species are met with a vigorous and destructive immune response (31). Given the reported immunomodulatory properties of bifidobacteria, our observation that *B. longum* serpin acts as an efficient inhibitor of HNE is of particular interest because the release of neutrophil elastase and other granule proteases by activated neutrophils at the sites of intestinal inflammation represent an important mechanism of innate immunity (32, 33). Massive recruitment and activation of neutrophils in the intestine are triggered during intestinal inflammation caused by pathogenic bacteria but can also be a result of a pathological immune activation as observed in the inflammatory bowel disease. Identification of a novel neutrophil elastase inhibitor produced by the commensal bacterium *B. longum* suggests an intriguing possibility that the release of a neutrophil elastase inhibitor at the sites of intestinal inflammation may be beneficial for reducing the deleterious effects of the HNE activity, similar to the way the pathological tissue damage associated with the excessive HNE activity is attenuated by α_1-antitrypsin, the physiological HNE inhibitor in the blood plasma. Further investigation of the *B. longum* adaptation mechanisms to the mammalian GIT is required for better understanding of the potential role of the *B. longum* serpin in the interaction of this bacterial species with its host.

REFERENCES

1. Gettins, P. G. (2002) *Chem. Rev.* **102,** 4751–4804
2. Silverman, G. A., Bird, P. I., Carrell, R. W., Church, F. C., Coughlin, P. B., Gettins, P. G., Irving, J. A., Lomas, D. A., Luke, C. J., Moyer, R. W., Pemberton, P. A., Remold-O'Donnell, E., Salvesen, G. S., Travis, J., and Whisstock, J. C. (2001) *J. Biol. Chem.* **276,** 33293–33296
3. Wei, A., Rubin, H., Cooperman, B. S., and Christianson, D. W. (1994) *Nat. Struct. Biol.* **1,** 251–258
4. Loebermann, H., Tokuoka, R., Deisenhofer, J., and Huber, R. (1984) *J. Mol. Biol.* **177,** 531–557
5. Huntington, J. A., Read, R. J., and Carrell, R. W. (2000) *Nature* **407,** 923–926
6. Hunt, L. T., and Dayhoff, M. O. (1980) *Biochem. Biophys. Res. Commun.* **95,** 864–871
7. Doolittle, R. F. (1983) *Science* **222,** 417–419
8. Wright, H. T., Qian, H. X., and Huber, R. (1990) *J. Mol. Biol.* **213,** 513–528
9. Irving, J. A., Steenbakkers, P. J., Lesk, A. M., Op den Camp, H. J., Pike, R. N., and Whisstock, J. C. (2002) *Mol. Biol. Evol.* **19,** 1881–1890
10. Schell, M. A., Karmirantzou, M., Snel, B., Vilanova, D., Berger, B., Pessi, G., Zwahlen,

M. C., Desiere, F., Bork, P., Delley, M., Pridmore, R. D., and Arigoni, F. (2002) *Proc. Natl. Acad. Sci. U. S. A.* **99,** 14422–14427
11. Roberts, T. H., Hejgaard, J., Saunders, N. F., Cavicchioli, R., and Curmi, P. M. (2004) *J. Mol. Evol.* **59,** 437–447
12. Irving, J. A., Cabrita, L. D., Rossjohn, J., Pike, R. N., Bottomley, S. P., and Whisstock, J. C. (2003) *Structure* **11,** 387–397
13. Fulton, K. F., Buckle, A. M., Cabrita, L. D., Irving, J. A., Butcher, R. E., Smith, I., Reeve, S., Lesk, A. M., Bottomley, S. P., Rossjohn, J., and Whisstock, J. C. (2005) *J. Biol. Chem.* **280,** 8435–8442
14. Furrie, E., Macfarlane, S., Kennedy, A., Cummings, J. H., Walsh, S. V., O'Neil D, A., and Macfarlane, G. T. (2005) *Gut* **54,** 242–249
15. O'Mahony, L., McCarthy, J., Kelly, P., Hurley, G., Luo, F., Chen, K., O'Sullivan G, C., Kiely, B., Collins, J. K., Shanahan, F., and Quigley, E. M. (2005) *Gastroenterology* **128,** 541–551
16. Bieth, J. G. (1980) *Bull. Eur. Physiopathol. Respir.* **16,** (suppl.) 183–197
17. Schechter, N. M., and Plotnick, M. I. (2004) *Methods* **32,** 159–168
18. Marvin-Guy, L., Lopes, L. V., Affolter, M., Courtet-Compondu, M.-C., Wagniere, S., Bergonzelli, G. E., Fay, L. B., and Kussmann, M. (2005) *Proteomics* **5,** 2561–2569
19. Marvin-Guy, L. F., Parche, S., Wagniere, S., Moulin, J., Zink, R., Kussmann, M., and Fay, L. B. (2004) *J. Am. Soc. Mass Spectrom.* **15,** 1222–1227
20. Altschul, S. F., Madden, T. L., Schaffer, A. A., Zhang, J., Zhang, Z., Miller, W., and Lipman, D. J. (1997) *Nucleic Acids Res.* **25,** 3389–3402
21. Irving, J. A., Pike, R. N., Lesk, A. M., and Whisstock, J. C. (2000) *Genome Res.* **10,** 1845–1864
22. Krogh, A., Larsson, B., von Heijne, G., and Sonnhammer, E. L. (2001) *J. Mol. Biol.* **305,** 567–580
23. Beatty, K., Bieth, J., and Travis, J. (1980) *J. Biol. Chem.* **255,** 3931–3934
24. Sziegoleit, A., Krause, E., Klor, H. U., Kanacher, L., and Linder, D. (1989) *Clin. Biochem.* **22,** 85–89
25. Shiga, Y., Yamagata, H., Tsukagoshi, N., and Udaka, S. (1995) *Biosci. Biotechnol. Biochem.* **59,** 2348–2350
26. Grenier, D. (1994) *FEMS Microbiol. Lett.* **119,** 13–18
27. Eggers, C. T., Murray, I. A., Delmar, V. A., Day, A. G., and Craik, C. S. (2004) *Biochem. J.* **379,** 107–118
28. Travis, J., and Salvesen, G. S. (1983) *Annu. Rev. Biochem.* **52,** 655–709
29. Isolauri, E., Kirjavainen, P. V., and Salminen, S. (2002) *Gut* **50,** Suppl. 3, III54–III59
30. Sartor, R. B. (2004) *Gastroenterology* **126,** 1620–1633
31. Sansonetti, P. J. (2004) *Nat. Rev. Immunol.* **4,** 953–964
32. Burg, N. D., and Pillinger, M. H. (2001) *Clin. Immunol.* **99,** 7–17
33. Reeves, E. P., Lu, H., Jacobs, H. L., Messina, C. G., Bolsover, S., Gabella, G., Potma, E. O., Warley, A., Roes, J., and Segal, A. W. (2002) *Nature* **416,** 291–297